Cancer Genetics 231–232 (2019) 1–13

Cancer Genetics

ORIGINAL ARTICLE

Multidisciplinary analysis of pediatric T-ALL: 9q34 gene fusions

Peter Papenhausen[a,*], Carla A. Kelly[a], Zhenxi Zhang[b], James Tepperberg[a], Rachel D. Burnside[a], Stuart Schwartz[a]

[a] *Laboratory Corporation of America, 1904 TW Alexander Drive, Research Triangle Park, NC 27709, United States;*
[b] *Laboratory Corporation of America, 3400 Computer Drive, Westborough, MA 01581, United States*

Abstract

T-cell acute lymphoblastic leukemia (T-ALL) is not as frequently reported as the B-cell counterpart (B-ALL), only occurring in about 15% of pediatric cases with a typically heterogeneous etiology. Approximately 8% of childhood T-ALL cases have rearrangements involving the *ABL1* tyrosine kinase gene at 9q34.12; although a t(9;22), resulting in a fusion of *ABL1* with the *BCR* gene at 22q11.23 is a common occurrence in B-ALL, it is not a typical finding in T-ALL. A subset of 10 of 40 documented cases of T-ALL analyzed over a 5-year period is presented, each having gene rearrangements within band 9q34 that resulted in fusions other than *BCR/ABL1*. These cases included fusions involving *ABL1, SET* (9q34.11), *NUP214* (9q34.13), *SPTAN1* (9p34.11), and *TNRC6B* (22q13.1). Among the 10 cases are: six *SET/NUP214* fusions, two *ABL1/NUP214* fusions (one of which was associated with episomal amplification) and novel *SPTAN1/ABL1* and *TNRC6B/ABL1* fusions. The evaluations of these clones were each significantly aided by FISH analysis, which directed subsequent microarray and anchored multiplex PCR testing for fusion confirmations.

Keywords T-cell acute lymphoblastic leukemia(T-ALL), Chromosome microarray analysis (CMA), Archer anchored multiplex PCR (AMP^{TM}), Fluorescence In Situ Hybridization (FISH), *ABL1*, *NUP214*.

Introduction

T-cell acute lymphoblastic leukemia (T-ALL) is less common than B-cell acute lymphoblastic leukemia (B-ALL) in pediatric as well as adult malignancies, comprising 15% of ALL cases in children and 25% of cases in adults [1]. However, the relative adverse outcome of T-ALL warrants special attention, with many pathogenic gene mutations having been identified. Rapid identification of clone specific subgroups is of primary importance for stratifying responses to treatment, with the ultimate goal of improving cure rates. Clinical lab evaluations typically include use of Fluorescence In Situ Hybridization (FISH), cytogenetics and cancer gene sequence analysis, as well as chromosome microarray analysis (CMA) and RNA sequencing for pathogenic fusions (Table 1). The focus of this study is to offer an efficient reflex model for the evaluation of pathogenic subsets of T-ALL with gene fusions involving *ABL1, NUP214* or both.

Materials and methods

The cases (40) were part of ongoing Children's Oncology Group (COG) ALL studies evaluated over a five-year period. All patient evaluations followed initial offsite immunophenotyping, which directed the type of ancillary FISH testing accompanying the G-band chromosome analyses. Only BCR/ABL1 FISH was required for COG T-ALL studies, but in some cases B-ALL panel probes, which include BCR/ABL1, were processed before the immunophenotyping was

Received October 19, 2018; received in revised form December 7, 2018; accepted December 8, 2018

* Corresponding author.
E-mail addresses: papenhp@labcorp.com, kellyc@labcorp.com, zhangz2@labcorp.com, tepperj@labcorp.com, burnsir@labcorp.com, schwas1@labcorp.com

2210-7762/$ - see front matter © 2018 Elsevier Inc. All rights reserved.
https://doi.org/10.1016/j.cancergen.2018.12.002

Table 1 Complete Cytogenetics, CMA, and FISH results.

Case number	Cytogenetics results	CMA results	Specific FISH probe results
1	45,X,-Y,?add(1)(p36.2),del(1)(q35), −5,del(11)(q23.1q23.3), + 17, der(17)t(5;17)(p12;p11.2)x2[*cp*16]/ 46,XY[4]	arr[hg19] 1p36.33p36.11(849,466–26,715,286)x1∼2, 2p22.2p21(37,089,587–43,289,540)x1∼2, 2p14p13.3(65,077,746–69,020,209)x1∼2 2p12(75,899,731–80,381,819)x1∼2, 5p15.33q11.2(113,576–53,294,970)x2∼3, 5q11.2q35.3(53,295,999–180,719,789)x1∼2 9q34.11q34.13(131,457,911–134,030,856)x1∼2, 10q21.3(67,436,887–69,833,498)x1∼2, 11p14.1p12(30,301,048–36,777,339)x1∼2, 11p13(32,242,706–32,589,152)x0∼2, 11q14.2q22.3(85,955,951–108,435,303)x1∼2 12p13.2p12.3(10,486,264–15,248,809)x1∼2, 17p13.3p11.1(525–22,227,470)x1∼2, 17q11.1q25.3(25,336,773–81,041,938)x2∼3, 19p13.3(3,319,780–4,178,464)x1∼2, 19p13.2(10,099,171–11,394,541)x1∼2, Xp11.3(44,194,398–45,079,718)x0∼1, (Y)x0∼1	**BCR/ABL1: ABNORMAL** nuc ish 9q34(*ASS1*)x1,(*ABL1*)x1,*ABL1* dim, 22q11.2(*BCR*x2)[193/200] **TCF3:NORMAL** nuc ish 19p13.3(*TCF3* × 2)[200] **CDKN2A:NORMAL** nuc ish 9p21(*CDKN2A*x2)[200] **KMT2A:NORMAL** nuc ish 11q23(KMT2Ax2)[200] **ETV6/RUNX1:ABNORMAL** nuc ish 12p13(*ETV6* × 1),21q22(*RUNX1* × 2)[195/200] **CHR 4, 10, 17:ABNORMAL** nuc ish 4cen(D4Z1 × 2),10cen(D10Z1 × 2), 17cen(D17Z1 × 3)[177/200]
2	No mitotic activity	arr[hg19] 9p24.3p13.1(192,128–40,087,758)x2 hmz (∼95%) 9p21.3(21,920,647–23,647,858)x0∼2 9q34.11q34.13(131,459,252–134,030,856)x1∼2 16p11.2q23.1(34,197,491–75,818,956)x1∼2 18p11.32p11.22(136,226–10,519,522)x1∼2	**BCR/ABL1: ABNORMAL** nuc ish 9q34(*ASS1,ABL1*)x1,22q11.2(BCRx2)[180/200] **TCF3:NORMAL** nuc ish 19p13.3(*TCF3* × 2)[200] **KMT2A:NORMAL** nuc ish 11q23(*KMT2A*x2)[200] **ETV6/RUNX1:NORMAL** nuc ish 12p13(*ETV6* × 2),21q22(*RUNX1* × 2)[200] **CHR 4, 10, 17:NORMAL** nuc ish 4cen(D4Z1 × 2),10cen(D10Z1 × 2), 17cen(D17Z1 × 2)[200]
3	46,XX	arr 9q34.11q34.13(131,456,252–134,025,284)x1∼2, 12p13.2p12.1(10,233,839–22,501,127)x1∼2, 12p12.1(23,725,896–24,307,463)x1∼2	***BCR/ABL1*: ABNORMAL** nuc ish 9q34(*ASS1,ABL1*)x1,22q11.2(*BCR*x2)[33/200]
4	46,XY	arr[hg19] 6q23.3(135,463,996–135,777,890)x2∼3 9p24.3p13.2(192,128–38,037,086)x2 hmz, 9p21.3(21,839,119–21,976,418)x0∼2, 9q34.11q34.13(131,457,917–134,030,856)x1∼2	**BCR/ABL1: ABNORMAL** nuc ish 9q34(*ASS1*)x1,(*ABL1*)x1,*ABL1* dim, 22q11.2(*BCR*x2)[175/200]

(*continued on next page*)

Table 1 (*continued*)

Case number	Cytogenetics results	CMA results	Specific FISH probe results
5	46,XX,add(1)(p12),−5, del(6)(q13q16),add(7)(q32),del(9)(q22q34), add(12)(p11.2),+mar[*cp*6]/46,XX[5]	arr[hg19] 1p36.33p36.11(849,466–26,895,802)x1∼2, 5q15q35.3(94,648,219–180,719,789)x1∼2, 6q12q16.1(65,825,662–94,968,843)x1∼2, 6q16.1q27(94,972,307–170,919,482)x2∼3, 7q31.1q36.3(110,204,303–159,119,707)x1∼2, 9q34.11q34.13(131,457,917–134,030,856)x1∼2, 12p13.33p11.22(173,786–29,511,593)x1∼2, 13q21.32q34(66,983,704–115,107,733)x2∼3, 14q11.2(20,511,672–22,913,412)x1∼2, 15q26.1q26.3(90,914,633–102,429,112)x2∼3	**BCR/ABL1: ABNORMAL (**nuc ish 9q34(*ASS1*)x1,(*ABL1*)x1,*ABL1* dim, 22q11.2(*BCR*x2)[174/200] **TCF3:NORMAL** nuc ish 19p13.3(*TCF3*×2)[200] **CDKN2A:NORMAL** nuc ish 9p21(*CDKN2A*x2)[200] **KMT2A:NORMAL** nuc ish 11q23(*KMT2A*x2)[200] **ETV6/RUNX1:ABNORMAL** nuc ish 12p13(*ETV6*×1),21q22(*RUNX1*×2)[48/200] **CHR 4, 10, 17:NORMAL** nuc ish 4cen(D4Z1×2),10cen(D10Z1×2), 17cen(D17Z1×2)[200]
6	47,XY,+4,del(12)(p11.2),add(12)(q24.1)[12]/ 46,XY[9]	arr[hg19] (4)x2∼3, 9q34.11q34.13(131,449,252–134,025,284)x1∼2, 12p13.2p11.22(10,233,839–28,574,258)x1∼2, 17q21.2q25.3(39,705,863–81,041,938)x2∼3, 19p13.3p11(260,912–24,507,141)x2 hmz, 19q11q13.43(28,271,017–59,128,982)x2 hmz	**BCR/ABL1: ABNORMAL** nuc ish 9q34(*ASS1,ABL1*)x1,22q11.2(*BCR*x2)[183/200] **KMT2A:NORMAL** nuc ish 11q23(*KMT2A*x2)[200] **ETV6/RUNX1:ABNORMAL** nuc ish 12p13(*ETV6*×1),21q22(*RUNX1*×2)[186/200] **CHR 4, 10, 17:ABNORMAL** nuc ish 4cen(D4Z1×3),10cen(D10Z1×2), 17cen(D17Z1×2)[177/200]
7	46,XX,del(5)(q31)[11]/46,XX[9]	arr[hg19] 1p36.13p36.11(17,471,570–25,773,345)x1∼2, 1p21.1p12(105,500,397–119,342,059)x1∼2, 5q22.1q32(111,215,480–149,728,347)x1∼2, 9p21.3(21,829,603–23,461,151)x1∼2, 9p21.3(21,936,324–21,981,583)x0∼2, 9q34.11q34.12(133,009,149–133,680,922)x1∼2, 9q34.12q34.13(133,681,014–134,108,056)x2∼4, 9q34.13(134,108,064–134,305,809)x1∼2, 17q11.2(29,192,714–29,531,181)x1∼2, 17q21.31(41,982,673–42,622,133)x1∼2, 17q21.31(42,517,551–42,622,133)x0∼2, 19p13.3p12(260,912–22,281,636)x2 hmz	**BCR/ABL1: ABNORMAL** nuc ish 9q34(*ASS1*)x1,(*ABL1*)x2,22q11.2(*BCR*x2)[143/200]

(*continued on next page*)

Table 1 (*continued*)

Case number	Cytogenetics results	CMA results	Specific FISH probe results
8	46,XY,del(6)(q21),−9,add(9)(p13), del(10)(q25),+mar[2]/46,XY[51]	arr{hg19} 2q36.3q37.1(229,824,321–232,686,378)x1∼2, 4q31.22(146,877,283–147,313,215)x1∼2, 5p15.32p15.31(6,146,533–7,046,905)x1∼2, 6p22.3(17,944,220–18,894,236)x1∼2, 6q14.1q21(78,496,362–109,837,934)x1∼2, (9)x2 hmz, 9p21.3(21,829,603–22,423,159)x0∼1, 9q34.12q34.13(133,670,110–134,098,219)x2∼12, 10q25.3q26.3(117,277,770–135,534,747)x1∼2, 12q24.23(118,654,166–118,879,833)x1∼2, 14q32.2(98,483,775–99,108,096)x1∼2, 19p13.3(3,798,824–4,424,084)x1∼2, 19p13.2(10,898,850–11,748,330)x1∼2, 19q13.33q13.43(49,956,911–59,128,983)x2∼4, 21q22.13q22.2(39,372,633–40,225,229)x1∼2	**BCR/ABL1: ABNORMAL** nuc ish 9q34(*ASS1*)x2,(*ABL1* amp), 22q11.2(*BCR*x2)[58/200]/nuc ish 9q34(*ASS1*)x4,(*ABL1* amp),22q11.2(*BCR*x2)[17/200] **TCF3:ABNORMAL (NO REARRANGEMENT)** nuc ish 19p13.3(*TCF3* × 4)[27/200] **CDKN2A:ABNORMAL** nuc ish 9p21(*CDKN2A*x0)[174/200] **KMT2A:ABNORMAL (NO REARRANGEMENT)** nuc ish 11q23(*KMT2A*x4)[27/200] **ETV6/RUNX1:ABNORMAL (NO FUSION)** nuc ish 12p13(*ETV6* × 4),21q22(*RUNX1* × 4)[37/200] **CHR 4, 10, 17:ABNORMAL** nuc ish 4cen(D4Z1 × 4),10cen(D10Z1 × 4), 17cen(D17Z1 × 4)[19/200]
9	47,XY,i(7)(q10),+8[16]/46,XY[4]	arr[hg19] 7p23p11.2(43,361–56,843,372)x1∼2, 7q11.21q34(63,189,414–159,119,707)x2∼3, (8)x2∼3, 9p24.3p21.1(192,129–33,194,815)x2 hmz (∼65%), 9p21.3(21,819,462–21,996,603)x0∼2, 9q34.11(131,334,816–133,735,644)x1∼2	**BCR/ABL1: ABNORMAL** nuc ish 9q34(*ASS1*)x1,(*ABL1* dim)x1,22q11.2(*BCR*x2)[70/100] **TCF3:NORMAL** nuc ish 19p13.3(*TCF3* × 2)[100] **KMT2A(MLL):NORMAL** nuc ish 11q23(*KMT2A*x2)[100] **ETV6/RUNX1:NORMAL** nuc ish 12p13(*ETV6* × 2), 21q22(*RUNX1* × 2)[100] **CHR 4, 10, 17:NORMAL** nuc ish 4cen(D4Z1 × 2),10cen(D10Z1 × 2), 17cen(D17Z1 × 2)[100]
10	46,XX	arr[hg19] 9p21.3(20,896,688–22,241,889)x1∼2, 9p21.3(21,617,251–22,193,687)x0∼2, 9q34.11q34.12(132,371,789–133,678,643)x1∼2, 14q32.2(98,551,356–99,783,405)x1∼2, 22q13.1(40,709,149–40,815,872)x1-2	**BCR/ABL1: ABNORMAL** nuc ish 9q34(*ASS1*)x1,(*ABL1*)x1,(*ABL1* dim)x2, 22q11.2(*BCR*x2)[192/200] **TCF3:NORMAL** nuc ish 19p13.3(*TCF3* × 2)[200] **CDKN2A(P16):ABNORMAL** nuc ish 9p21(*CDKN2A*x0)[187/200] **KMT2A(MLL):NORMAL** nuc ish 11q23(*KMT2A*x2)[200] **ETV6/RUNX1:NORMAL** nuc ish 12p13(*ETV6* × 2),21q22(*RUNX1* × 2)[200] **CHR 4, 10, 17:NORMAL** nuc ish 4cen(D4Z1 × 2),10cen(D10Z1 × 2), 17cen(D17Z1 × 2)[200]

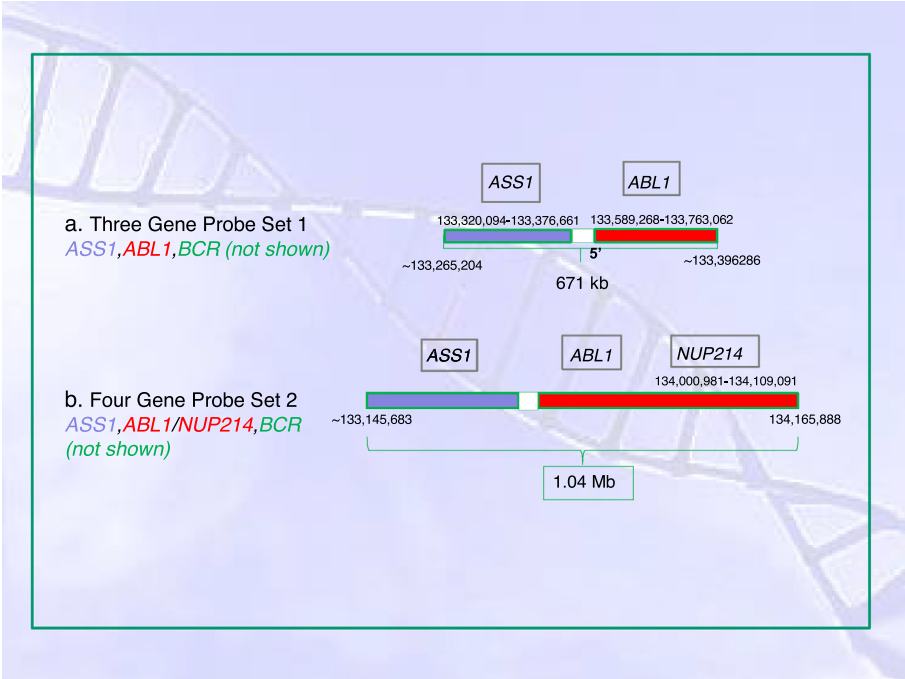

Fig. 1 *9q34 FISH Probe Sets [hg19].* (a) Probe set 1 targeting the *ASS1* control site labeled in blue and *ABL1* labeled in red (green *BCR* not present in diagrams). (b) Probe set 2 with same color specificity, but the *ABL1* site extends through the adjacent *NUP214* gene. (For interpretation of the references to colour in this figure legend, the reader is referred to the web version of this article.)

completed. Analyses included use of CytoScan HD® CMA in all 10 cases that were added based on abnormal 9q34 targeted FISH results to determine the precise DNA copy number changes and to identify potential gene fusion partners [2].

Archer Anchored Multiplex PCR (AMP™) analysis, a form of next-generation sequencing (NGS), using an 87-gene panel was additionally performed on nine of the cases to confirm the gene fusions. AMP™ permits gene rearrangements to be rapidly detected by next generation sequencing, using RNA isolated from DNA remaining after completion of CMA. The process involves fragmentation, end repair, and ligation, followed by two rounds of PCR performed at low cycles [3].

The FISH was done using two different commercial BCR/ABL1 probe sets, each with an *ABL1* linked control site gene target (*ASS1*). The difference between the probe sets is that probe set 1 (PS#1, Abbott Molecular Company) detects only the three genes while probe set 2 (PS#2, Kreatech, Leica BioSystems) has combined specificity for *ABL1* and the adjacent *NUP214* gene (Fig. 1).

Results

Of the ten cases presented (Table 2), the six cases with *SET/NUP214* fusions were initially identified because of deletions of the *ABL1/ASS1* gene targets in routine BCR/ABL1 FISH analysis and CMA was performed to determine gene involvement. Depending on the probe set that was used (Fig. 1), either complete loss of *ABL1* was noted (PS#1) or partial loss of the combined *ABL1/NUP214* signal (PS#2) was seen (Fig. 2). The CMAs each showed an interstitial deletion of the ~2.6 Mb region between the *SET* and *NUP214* genes that truncated both genes (Fig. 3). A fusion of the genes was confirmed by subsequent AMP™ sequencing in all 6 cases, involving exon 7 of *SET* and exons 17–18 of *NUP214*. Four of these six cases also demonstrated *ETV6* deletions in the CMA analyses, while none of four cases with other fusions showed this loss. *CDKN2A* deletions were found in 2 of the 6 *SET/NUP214* cases and all 4 of the other fusion cases.

The FISH result for Case 7 again showed a loss of the control *ASS1* signal, but there appeared to be no change in the dual *ABL1/NUP214* signal using PB#2 (Fig. 4). The reflexed CMA showed a duplication of the region between *ABL1* and *NUP214*, in addition to two small flanking deletions that truncated the two genes centromeric to *ABL1* and telomeric to *NUP214* (Fig. 5a). A schematic of the deletions and duplication are presented in Fig. 5b. The region of signal loss is approximately the same size as the gain from the duplication, resulting in a normal sized signal. Sequencing confirmed a fusion of exon 2 of *ABL1* and exon 34 of *NUP214*.

The FISH result in Case 8 was the only case of this cohort in which the *ASS1* control site was not deleted, revealing apparently normal homologue labeling in interphase analysis, but showing extensive nuclear dispersed amplification of the dual *ABL1/NUP214* signal using PS#2 (Fig. 6). The subsequent CMA confirmed a 12 copy number average amplification of the same region as patient 7. This is consistent with a circular fusion and episomal amplification of the *ABL1* and *NUP214* genes, characteristic of double minutes (dmins). The small size of the amplicon is well below G-band resolution, so they were not seen in the clonal karyotype. In addition, the single nucleotide polymorphism (SNP) based CMA showed copy neutral loss of heterozygosity (CN-LOH) for all of chromosome 9, with homozygous deletion of the

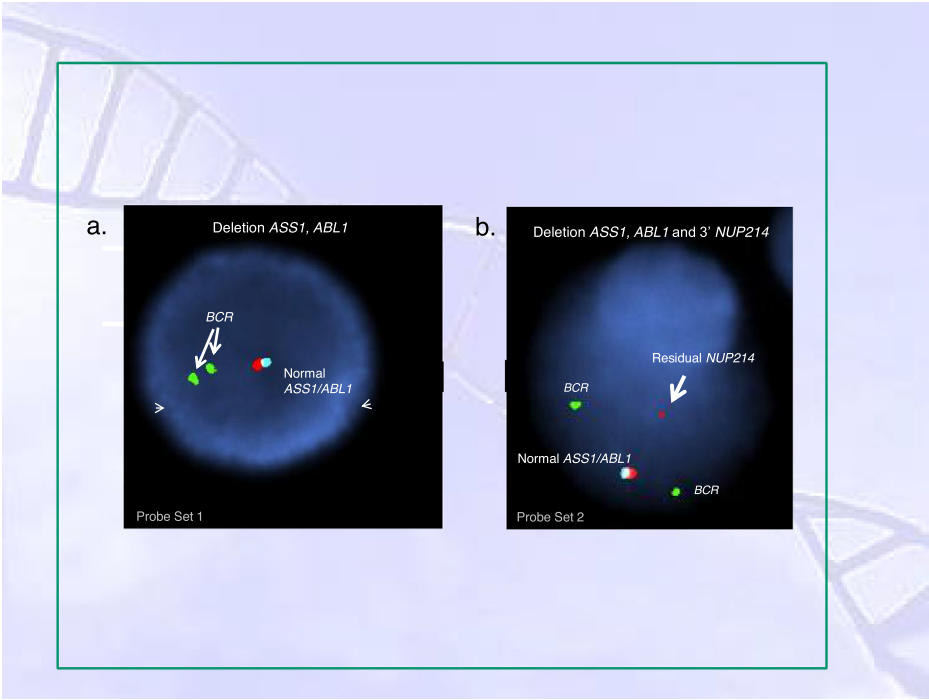

Fig. 2 *FISH in SET/NUP214 Fusion Cases.* (a) FISH displaying loss of *ASS1/ABL1* using probe set 1. (b) Loss of ASS1 with a diminished *ABL1/NUP214* signal, representing the residual 5′ NUP214 with probe set 2.

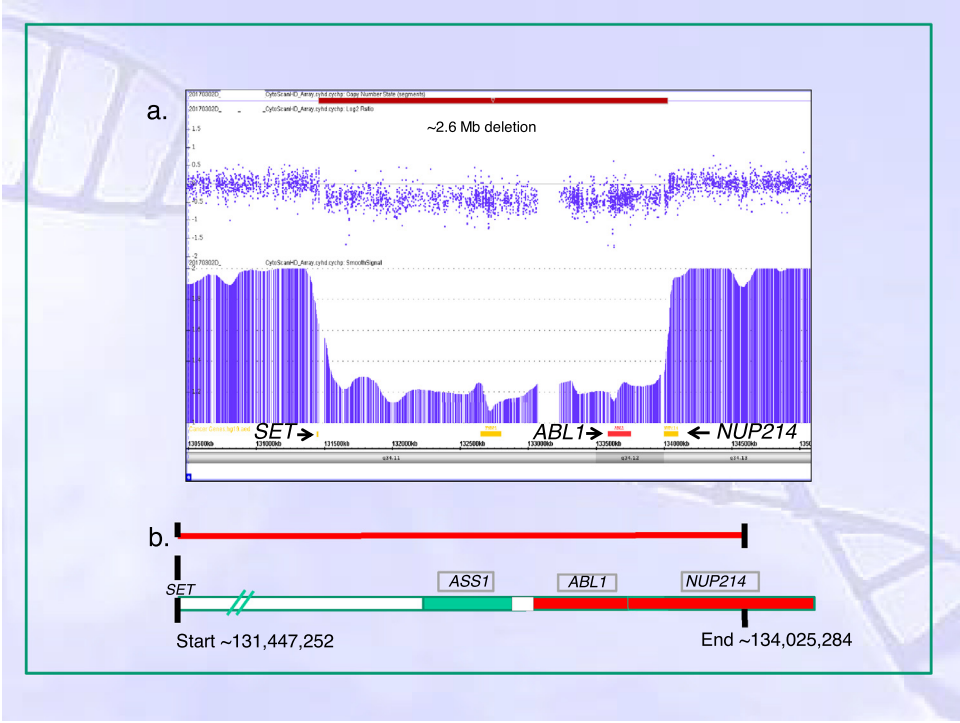

Fig. 3 *Deletion/Fusion of SET/NUP214.* Representative microarray from one of Cases 1–6 with the 2.6 Mb interstitial deletion and partial loss of *SET* and *NUP214*. Dotted graph shows the log 2 dosage of the regional probe targets and the bar graph depicts the average dosage of those targets (~1.2 copy number or 80% clonal involvement). (b) The fusion was confirmed by AMP™.

Table 2 Specific 9q34 FISH, CMA and AMP™ results.

Case number	Patient age (yrs)	Probe Set (PS) used: FISH result ('-': deleted; dim: diminished signal)	9q34 region (as determined by CMA)	Fusion genes	AMP™ coordinates	Other oncology-related genes lost
1	14	PS#2: *ASS1*-, *ABL1* & *NUP214* dim	(131,457,911–134,030,856)x1∼2	*SET* & *NUP214*	*SET* (131,456,321); *NUP214* (134,027,123)	*WT1* (hmz[a]), *ETV6, TP53, KDM6A, NF1*
2	8	PS#1: *ASS1*-, *ABL1*-	(131,459,252–134,030,856)x1∼2	*SET* & *NUP214*	*SET* (131,456,321); *NUP214* (134,027,123)	*CDKN2A* (hmz[a])
3	13	PS#1: *ASS1*-, *ABL1*-	(131,456,252–134,025,284)x1∼2	*SET* & *NUP214*	*SET* (131,456,321); *NUP214* (134,027,123)	*ETV6* (hmz[a])
4	10	PS#2: *ASS1*-, *ABL1* & *NUP214* dim	(131,457,917–134,030,856)x1∼2	*SET* & *NUP214*	*SET* (131,456,319); *NUP214* (134,034,770)	*CDKN2A* (hmz[b]), *MYB*
5	4	PS#2: *ASS1*-, *ABL1* & *NUP214* dim	(131,457,917–134,030,856)x1∼2	*SET* & *NUP214*	*SET* (131,456,321); *NUP214* (134,034,770)	*ETV6, MYB*
6	17	PS#1: *ASS1*-, *ABL1*-	(131,449,252–134,025,284)x1∼2	*SET* & *NUP214*	*SET* (131,456,321); *NUP214* (134,027,122)	*ETV6*
7	6	PS#2: *ASS1*-	(133,009,149–133,680,922)x1∼2, (133,681,014–134,108,056)x2∼3, (134,108,056–134,305,809)x1∼2	*ABL1* & *NUP214*	*ABL1* (134,106,156); *NUP214* (133,729,451)	*CDKN2A* (hmz[a]), *NF1*
8	10	PS#2: Amplification of *ABL1* & *NUP214*	pter-133,670,110)x1∼2, 133,670,110–134,098,219)x2∼12, (134,098,219-qter)x1∼2	*ABL1* & *NUP214*	NA	*CDKN2A* (hmz[b]), *DEK, SMARCA4, FOXO3, SH3GL1, ERG*
9	7	PS#1: *ASS1*-, *ABL1* dim	(131,334,816–133,735,644)x1∼2	*SPTAN1* & *ABL1*	*SPTAN1* (131,329,256); *ABL1* (133,738,149)	*CDKN2A* (hmz[b])
10	3	PS#2: *ASS1*-, *ABL1* & *NUP214* dim and distal to *BCR*	(132,371,789–133,678,643)x1∼2, 22q13.1(40,709,149–40,815,872)x1∼2	*TNRC6B* & *ABL1*	*TNRC6B* (40,709,001); *ABL1* (133,729,451)	*CDKN2A* (hmz[a])

[a] Homozygous.
[b] Homozygous secondary to Copy Neutral-Loss of Heterozygosity.

CDKN2A gene region from 9p (Fig. 7). CN-LOH in CMA analysis is shown by an alteration of the normal 1:1 allele specific dosage ratio of heterozygous SNPs. *CDKN2A* gene-targeted FISH is not required by COG, but was performed in some cases; homozygous loss was detected in 6 of the 10 CMA analyses.

Novel gene fusions detected in Cases 9 and 10 were again first suggested by abnormal FISH results that were reflexed to CMAs, which showed interstitial deletions. FISH using PS#1 in Case 9 showed a diminished *ABL1* signal, indicating a partial deletion, and loss of *ASS1* (Fig. 8). The deletion produced an apparent intra-chromosomal *SPTAN1/ABL1* gene fusion, consistent with an intervening *ASS1* gene loss (Fig. 9a). The AMP™ follow-up confirmed the novel fusion (Fig. 9b) of exon 2 of *SPTAN1* and exon 2 of *ABL1*.

The novel rearrangement in Case 10 had only the *ASS1* control site deleted with no apparent change in the *ABL1/NUP214* signal using PS#2. The CMA showed a 9q34 interstitial deletion which again spanned the *ASS1* gene site and included partial loss of 5′ *ABL1*, though no gene was apparent at the centromeric end of the deletion that would suggest a fusion partner. The AMP™ results subsequently identified fusion of *ABL1* with the *TNRC6B* gene, consistent with the metaphase BCR/ABL FISH which showed an apparent translocation of the residual *ABL1* signal distal to the *BCR* gene signal on chromosome 22 at the approximate locus of the *TNRC6B* gene (Fig. 10). The CMA analysis also showed a deletion of part of the *TNRC6B* gene and a small region distal to the gene at the approximate site of the *ABL1* FISH signal (Fig. 11).

Discussion

All 10 of the cases presented contained gene fusions that were cryptic by routine G-band chromosome analysis and the abnormal karyotypes found in 6 of the evaluations lacked an association with currently known ALL alterations. All but Case 8, characterized by episomal amplification, showed a deletion of the *ABL1* control site (*ASS1)* in the preliminary FISH analysis. The *ASS1* loss in standard BCR/ABL1 FISH

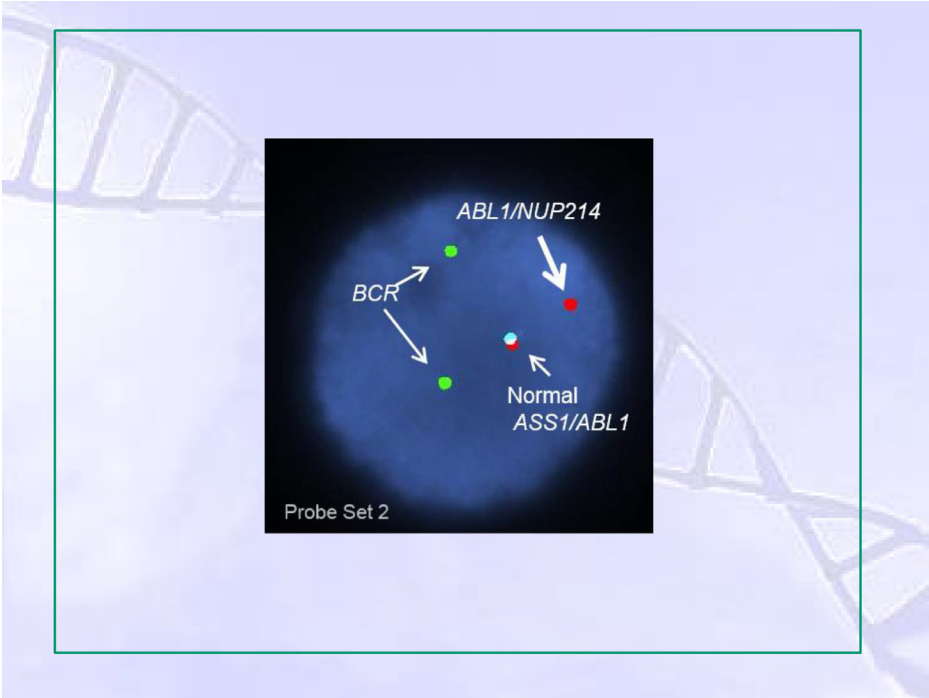

Fig. 4 *Case 7*, *ABL1/NUP214 Fusion*. Deletion of *ASS1* with no visible change in the size of the *ABL1/NUP214* signal using probe set 2.

screening of childhood T-ALL has, therefore, served as an impetus to ancillary CMA and/or RNA sequencing that has revealed a subgroup of gene fusion-mediated clones that involve either *NUP214* or *ABL1*, or both. Since the type of probe set used significantly alters the resulting *ABL1* or combined *ABL1/NUP214* signal, attention should be given to the related signal intensity of this target. For the most common *SET/NUP214* fusions, the ASS1 control was deleted using either probe set. However, when using PS#1, the *ABL1* signal was completely lost while a markedly diminished signal

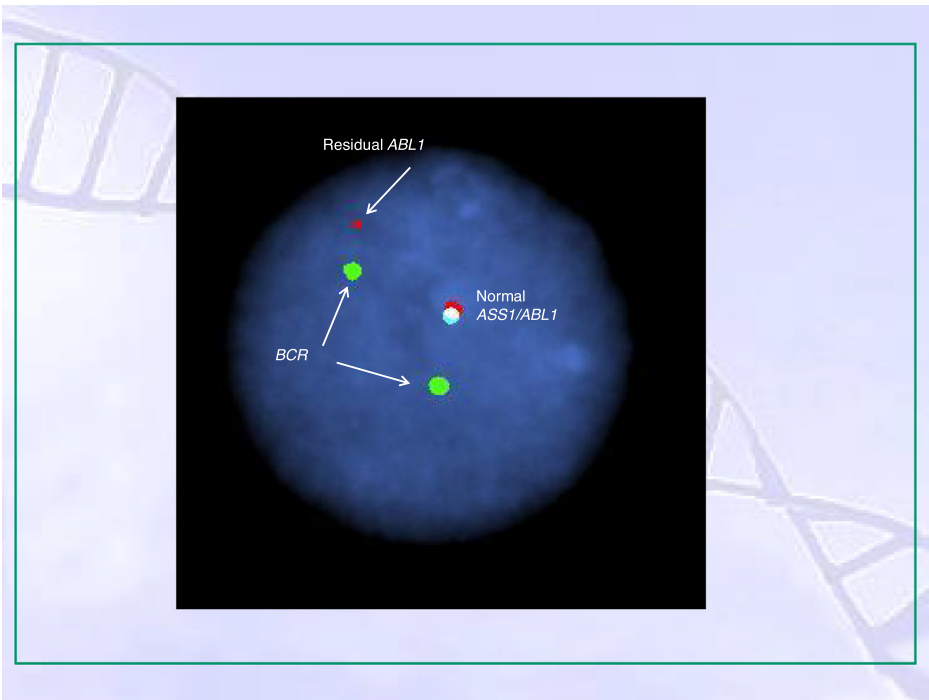

Fig. 8 *FISH of SPTAN1/ABL1 fusion in Case 9.* Using probe set 1, a loss of the *ASS1* control site and a diminished ABL1 signal were observed.

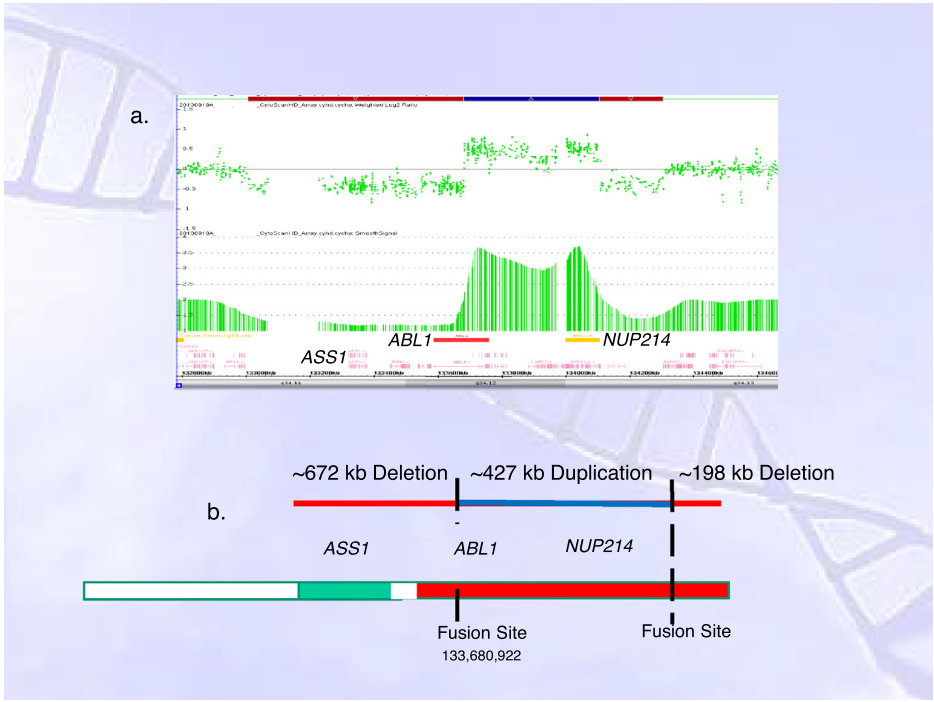

Fig. 5 *CMA of Case 7*. (a) Flanking/truncating deletions of *ABL1* and *NUP214* are apparent, along with duplication of the intervening region between the genes that resulted in an exon 2 ABL1 – exon 34 *NUP214* fusion, as indicated by AMP™ analysis (b).

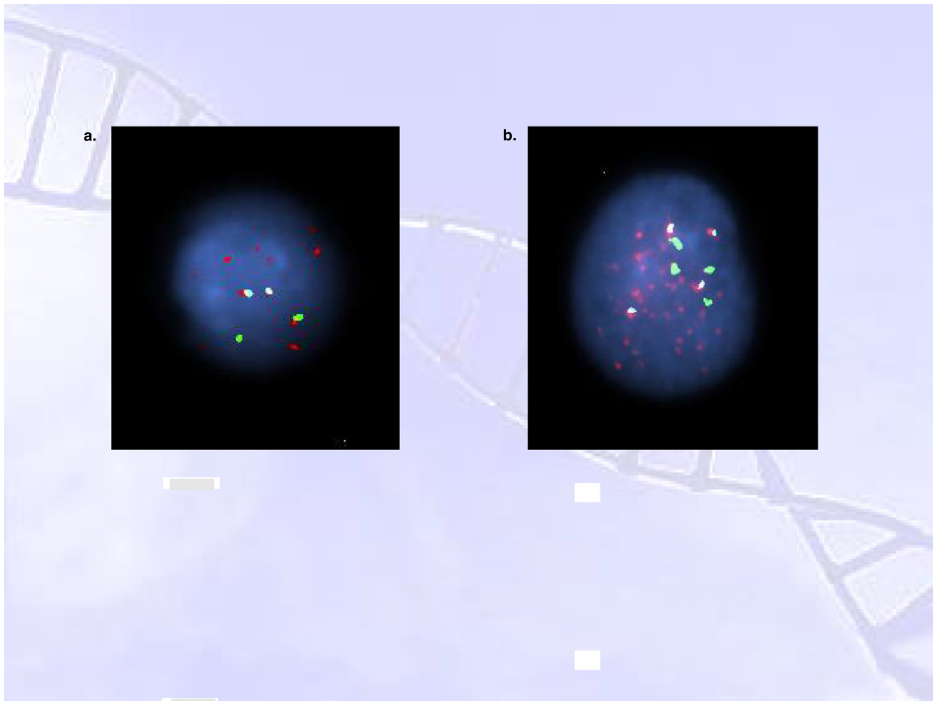

Fig. 6 *FISH and CMA showing ABL1/NUP214 dmins in Case 8*. Although the dmins are not visible in G-band analysis, interphase FISH reveals the diffuse (red) amplicons present in both the original clone with 2 copies of the ASS/ABL1/NUP214 linked signals and BCR (a) and the evolving tetraploid sub-clone with doubling of those signals (b). (For interpretation of the references to colour in this figure legend, the reader is referred to the web version of this article.)

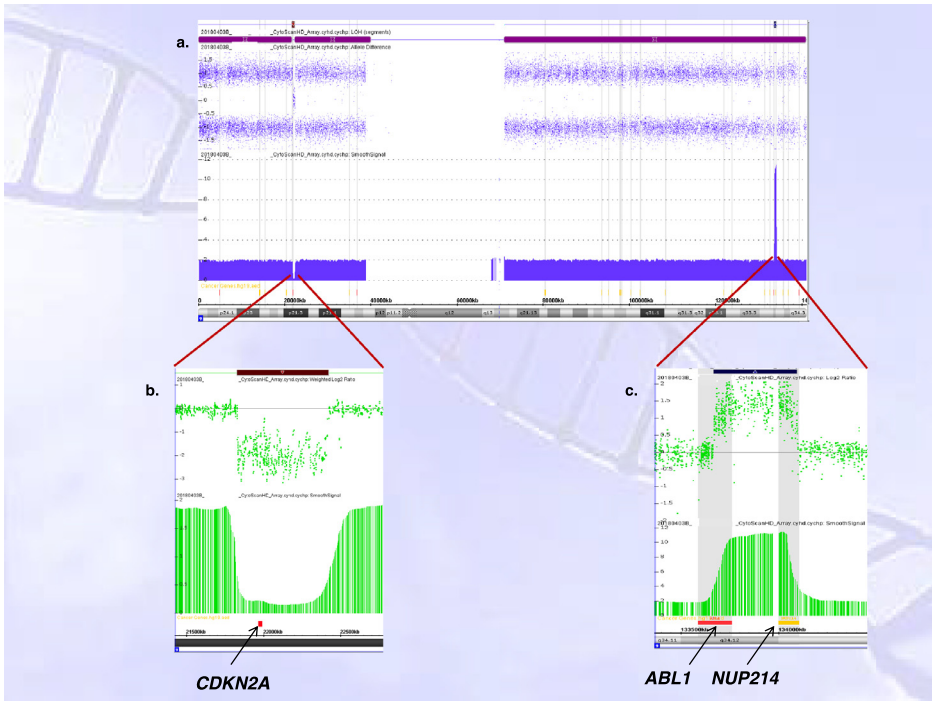

Fig. 7 *CMA of Chromosome 9 from Case 8.* (a) The chromosome 9 homologues with no evidence of heterozygosity (no tracts between the+1 and −1 allele dosage). (b) Homozygous loss of *CDKN2A*. (c) The amplified region present in the dmins, extending from intragenic ABL1 to intragenic NUP214 with the Y axis showing an average copy number/cell of ∼11.

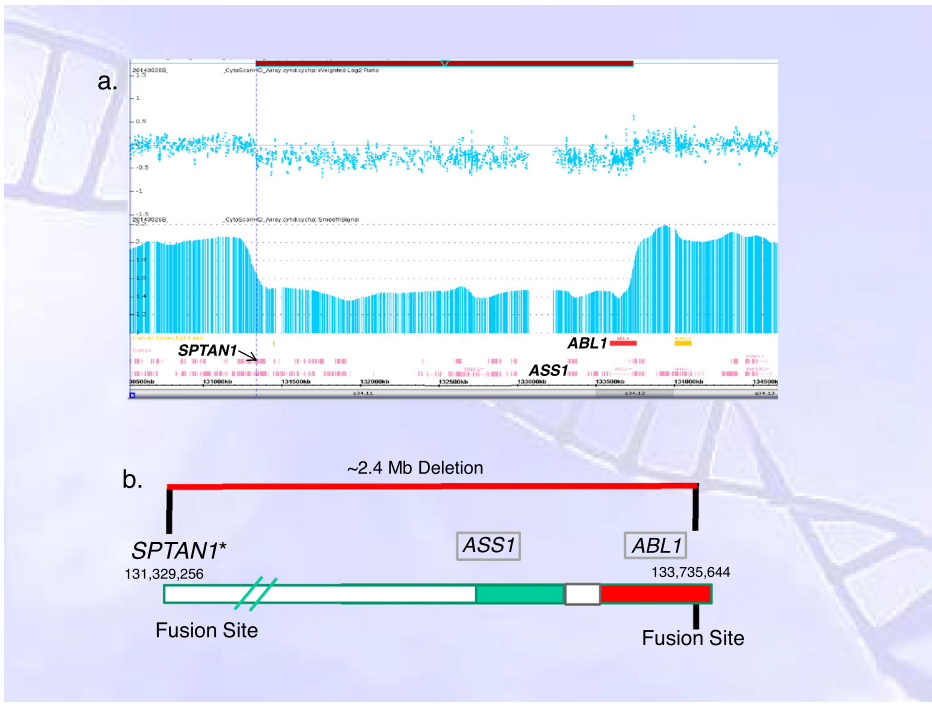

Fig. 9 *CMA of Case 9.* (a) The 2.4 Mb deletion truncating the *SPTAN1 and ABL1* genes is shown with clonal equivalent dosage of ∼60%. (b) Schematic of the deletion, with the *SPTAN1* gene at the proximal end of the deletion and ABL1 distal as identified by CMA. The gene fusion was confirmed as a fusion by AMP™.

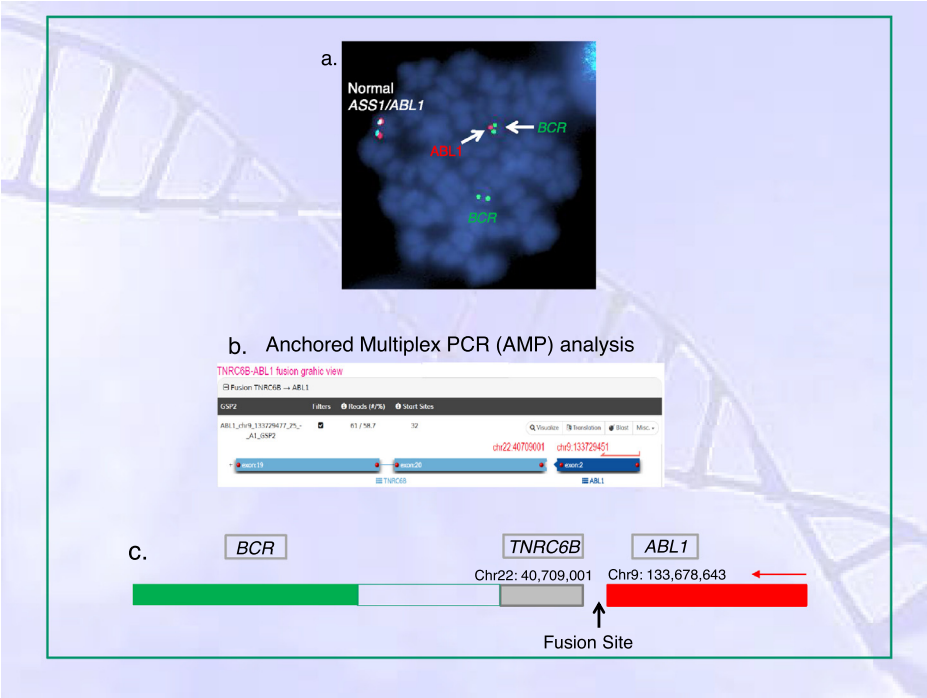

Fig. 10 *ABL1/TNRC6B Fusion in Case 10.* FISH performed with probe set 2 showed loss of the *ASS1* control site and 3′ *ABL1* from chromosome 9. The 5′ end of *ABL1* is translocated distal to *BCR* on chromosome 22. (b) Follow-up AMP™ testing identified the *TNRC6B* gene (locus 22q13.1) as the fusion partner for *ABL1*. (c) Schematic of the novel gene fusion with corresponding probe colors.

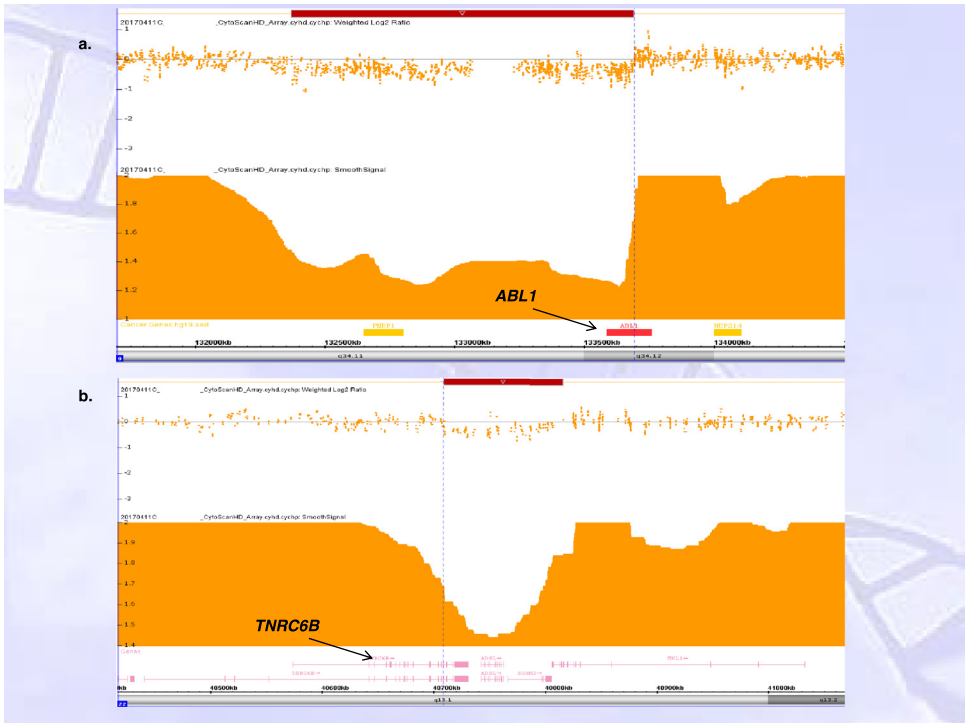

Fig. 11 *CMA of Case 10.* (a) CMA shows loss of *ABL1* (linked ASS1 control also deleted) that had no candidate fusion gene on the proximal end of the 9q deletion. (b) A small deletion involving the 3′ end of *TNRC6B* can also be seen consequent to the rearrangement.

was evident using PS#2 with only the residual *NUP214* signal remaining, offering an excellent clue to these fusions.

Although CMA cannot identify balanced rearrangements, it can be particularly effective in identifying the partner genes whenever there are copy number changes associated with unbalanced translocation derivatives or gene fusions. These conditions arise when there is a duplication of a translocation derivative or, as in most of the cases in this report, whenever there is a deletion or amplification associated with a gene fusion. The CMA analyses showed similar intragenic splice sites for the 6 patients with *SET/NUP214* gene fusions estimated at [hg19] chr9:131,459,252- 134,025,284. The RNA sequencing showed a *SET* splice site at 131,456, 321 in all cases and either 134,027,123 or 134,034,770 in *NUP214*. The cytogenetically cryptic interstitial ~2.6 Mb deletion that results in the *SET/NUP214* fusion has previously been described in T-ALL [4] and was the most common (6/10) in this cohort. Although all cases in this study were T-ALL related, there is evidence that some *SET/NUP214* fusions are not restricted to T-ALL [5–6].

The *ABL1/NUP214* fusions present in Cases 7 and 8 were very different in the initial FISH analyses. The episomal amplification seen in Case 8 has been more commonly reported in pediatric cases in the literature with fusion of these genes. This amplification is reported in about 5–6% of T-ALL [7–9]. The dmins present are below cytogenetic resolution due to the small size of the circular fusion amplicon, but are visible by FISH or molecular analysis. The *ABL1/NUP214* fusion was only associated with a single copy gain in the CMA analysis of Case 7, with metaphase FISH confirming that the duplicated segment remained *in situ.* Since the two copies are known to be fused, a tandem orientation may be presumed necessary, with the flanking deletions apparently facilitating the rearrangement.

Flanking deletions have also been reported in association with excised and amplified *MYC*-bearing dmins [10]. As opposed to the *MYC*-bearing dmins, which appear to offer clonal selective advantage from extra *MYC* dosage, the dmins in *ABL1/NUP214* fusion clones offer apparent selective advantage from amplified fusion products. A previous CMA of a case with *ABL1/NUP214* episomal amplification [5] showed only a small distally flanking deletion that included the residual 3′ end of the *NUP214* gene, but showed no proximal flanking deletion; the residual 5′ end of the *ABL1* gene and the more proximal *ASS1* gene were retained. Therefore, although the loss of the *ASS1* FISH control site signal common to the other cases reported in this cohort will not always be seen in *ABL1/NUP214* fusion clones, the typically numerous *ABL1* episomal amplification signals would be clear in FISH analysis regardless of which probe set is used. However, in a clone with an *in-situ* duplication-fusion of *ABL1/NUP214* without the flanking deletion of the *ASS1* gene, use of the combined *ABL1/NUP214* signal (PS#2) may not provide an abnormal result indicating the need to follow-up with further diagnostic molecular studies, such as CMA or AMP™. Since the overall size of the truncated but duplicated *ABL1/NUP214* fused gene targets in Case 7 did not significantly change, there was no apparent signal difference in the FISH analysis using the combined *ABL1/NUP214* targeted probe. Although not tested, the single targeted PS#1 *ABL1* FISH probe may have shown a bipartite signal in interphase analysis, offering a clue to pursue CMA or AMP™ confirmation.

Most episomal *ABL1/NUP214* fusion amplifications in the literature are generated after excision from one of the chromosome 9 homologues [11]. The CMA in Case 8 showed episomal *ABL1/NUP214* amplification along with homozygous *CDKN2A* deletion and CN-LOH of the entire chromosome, consistent with complete loss of the chromosome 9 homologue that generated the episome and duplication of the other CDKN2A deleted homologue. This interpretation is consistent with metaphase FISH that showed *CDKN2A* deleted and normal copies of *ASS1/ABL1/NUP214* in both homologues. Selective advantage driven single homologue deletions (or mutations) often evolve to homozygosity when there is mitotic recombination in the chromosome arm proximal to the deletion (or mutation) [12]. Whole chromosome loss and duplication of the remaining abnormal homologue is less common than mitotic recombination of a single arm. Biallelic *CDKN2A* loss appears to be common in T-ALL [13,14] and was noted in 6 of the 10 cases either through CN-LOH (Cases 4, 8, and 9) or homozygous deletions observed by FISH (Cases 2, 7, and 10). Multiple additional deletions were present in both Cases 7 and 8. Case 8, with the amplified *ABL1* episomal clone, showed the greatest number of neoplasia-related gene deletions with 6 (*NF1, DEK, SMARCA4, FOXO3, SH3GL1*, and *ERG*). The *NUP214* exons involved in fusions with *ABL1* have been variable in the published studies, ranging from 23–34 (34 in this case); exon 2 found in Case 7 is the common site in *ABL1* (Case 8 was not AMP™ sequenced).

Case 9 demonstrated a diminished *ABL1* signal (PS#1) and loss of the *ASS1* signal, consistent with an interstitial 9q34 deletion. The CMA for Case 9 showed an interstitial deletion between the *SPTAN1* and *ABL1* genes that truncated each, along with an additional 5q deletion seen by both G-band and CMA that is much more common in myeloid clones. This fusion does not appear to have been previously reported, thus, the confirmatory AMP™ was important. The splice site in *ABL1* was in the common exon 2 and exon 2 of *SPTAN1*. Deficiencies in alpha II spectrins, of which SPTAN1 is a member, have been shown to be associated with a defect in cell proliferation [15], but little is known relating to oncogenesis.

The *ASS1* deletion in Case 10 was not accompanied by a visible change in the *ABL1/NUP214* signal in the initial FISH analysis. Although the CMA clearly showed loss of 3′*ABL1*, a candidate gene at the other end of the deletion was lacking. The AMP™ analysis in this case was then especially important to identify the fusion partner, *TNRC6B*. The fusion involved exon 20 of *TNRC6B* and, again, exon 2 of *ABL1* and, as the other related *ABL1* fusions, may be sensitive to tyrosine kinase inhibitors. The metaphase FISH, consistent with loss of the 3′*ABL1*, showed no signal at 9q34 and the residual 5′*ABL1/NUP214* signal translocated distal to *BCR,* near the *TNRC6B* locus on chromosome 22. Only after the AMP™ identification of the fusion gene was a small interstitial deletion of the *TNRC6B* gene (107 Kb) noticed in the CMA. While deletions can be found at or near the break points of some reciprocal translocations, they have not been commonly seen in more than 2000 leukemia cases studied in this laboratory. The *TNRC6B* gene has been associated with gene expression [16] and mutations of the gene have been noted in liver cancer [17], while SNP susceptibility correlations have been seen in pediatric ALL [18] and uterine leiomyoma [19].

In summary, multidisciplinary analysis was necessary to identify the primary alterations present in these pediatric T-ALL cases. The cohort of 10 cases with either *ABL1* or *NUP214* rearrangements represent 25% (10/40) of all pediatric T-ALL patients analyzed. Only one T-ALL case positive for a *BCR/ABL1* fusion was found during this 5-year period. All fusions were mutually exclusive. Thus, these fusion subgroups have a significant incidence for which this follow-up protocol can be particularly helpful in the sub-classification of childhood T-ALL. Modern testing strategy has evolved to NGS because many mutations can be studied in a single assay; however, most NGS technology is limited in its ability to detect fusions. The ability to rapidly detect fusion partners is increasingly important for patient-specific treatment. No additional fusion testing by either CMA or AMP™ was performed on T-ALL samples with normal BCR/ABL FISH results, allowing significant savings of time and resources in the evaluations.

This research did not receive any specific grant from funding agencies in the public, commercial or not-for-profit sectors.

Conflict of interest statement

I have nothing to disclose other than I am an employee of Laboratory Corporation of America.

References

[1] Chiaretti S, Foa R. T-cell acute lymphoblastic leukemia. Haematologica 2009;94(2):160–2. doi:10.3324/haematol.2008.004150.

[2] Papenhausen P, Schwartz S, Risheg H, Keitges E, Gadi I, Burnside RD, et al. UPD detection using homozygosity profiling with a SNP genotyping microarray. Am J Med Genet A 2011;155:757–68. doi:10.1002/ajmg.a.33939.

[3] Zheng Z, Liebers M, Zhelyazkova B, Cao Y, Panditi D, Lynch KD, et al. Anchored multiplex PCR for targeted next-generation sequencing. Nat Med 2014;20(12):1479–84. doi:10.1038/nm/3729.

[4] Van Vlierberghe P, van Grotel M, Tchinda J, Lee C, Beverloo HB, van der Spek PJ, et al. The recurrent *SET-NUP214* fusion as a new *HOXA* activation mechanism in pediatric T-cell acute lymphoblastic leukemia. Blood 2008;111(9):4668–80. doi:10.1182/blood-2007-09-111872.

[5] Duployez N, Guillaume G, Ducourneau B, Fuentes MA, Grardel N, Boyer T, et al. *NUP 214-ABL1* fusion defines a rare subtype of B-cell precursor acute lymphoblastic leukemia that could benefit from tyrosine kinase inhibitors. Haematologica 2016;101(4):e133–4. doi:10.3324/haematol.2015.136499.

[6] Quentmeier H, Schneider B, Rohrs S, Romani J, Zaborski M, Macleod RA, Drexler HG. *SET-NUP214* fusion in acute myeloid leukemia and T-cell acute lymphoblastic leukemia-derived cell lines. J Hemat Oncol 2009;2(3):1–5. doi:10.1186/1756-8722-2-3.

[7] De Keersmaecker K, Porcu M, Cox L, Girardi T, Vandepoel R, de Beeck JO, et al. *NUP214-ABL1*-mediated cell proliferation in T-cell acute lymphoblastic leukemia is dependent on the LCK kinase and various interactingproteins. Haematologica 2014;99(1):85–93. doi:10.3324/haematol.2013.088674.

[8] Zhou MH, Yang QM. *NUP214* fusion genes in acute leukemia (Review). Oncol Lett 2014;8(3):959–62. doi:10.3892/ol.2014.2263.

[9] Graux C, Cools J, Melotte C, Quentmeier H, Ferrando A, Levine R, et al. Fusion of *NUP214* to *ABL1* on amplified episomes in T-cell acute lymphoblastic leukemia. Nat Genet 2004;36(10):1084–9. doi:10.1038/ng1425.

[10] Poddighe PJ, Wessels H, Merle P, Westers M, Bhola S, Loonen A, et al. Genomic amplification of *MYC* as double minutes in a patient with APL-like leukemia. Mol Cytogen 2014;7:67. doi:10.1186/s13039-014-0067-6.

[11] Hagemeijer A, Graux C. *ABL1* rearrangements in T-cell acute lymphoblastic leukemia. Gene Chromos Canc 2010;49(4):299–308. doi:10.1002/gcc.20743.

[12] Tischfield JA. Loss of heterozygosity or: How I learned to stop worrying and love mitotic recombination. Am J Hum Genet 1997;61(5):995–9. doi:10.1086/301617.

[13] Sulong S, Moorman AV, Irving JAE, Strefford JC, Konn ZJ, Case MC, et al. A comprehensive analysis of the *CDKN2A* gene in childhood acute lymphoblastic leukemia reveals genomic deletion, copy number neutral loss of heterozygosity, and association with specific cytogenetic subgroups. Blood 2009;113(1):100–7. doi:10.1182/blood-2008-07-166801.

[14] Karman K, Castor A, Behrendtz M, Forestier E, Olsson L, Ehinger M, et al. Deep sequencing and SNP array analyses of pediatric T-cell acute lymphoblastic leukemia reveal *NOTCH1* mutations in minor subclones and a high incidence of uniparental isodisomies affecting *CDKN2A*. J Hematol Oncol 2015;8:42. doi:10.1186/s13045-015-0138-0.

[15] Metral S, Machnicka B, Bigot S, Colin Y, Dhermy D, Lecomte MC. Alpha II-spectrin is critical for cell adhesion and cell cycle. J Biol Chem 2009;284(4):2409–18. doi:10.1074/jbc.M801324200.

[16] Liu J, Liu Z, Corey DR. The requirement for GW182 scaffolding protein depends on whether argonaute is mediating translation, transcription of splicing. Biochemistry 2018;57(35):5247–56. doi:10.1021/acs.biochem.8b00602.

[17] Li X, Xu W, Kang W, Wong SH, Wang M, Zhou Y, et al. Genomic analysis of liver cancer unveils novel driver genes and distinct prognostic features. Theranostics 2018;8(6):1740–51. doi:10.7150/thno.22010.

[18] Gutierrez-Camino A, Lopez-Lopez E, Martin-Guerrero I, Pinon MA, Garcia-Miguel P, Sancez-Toledo J, et al. Noncoding RNA-related polymorphisms in pediatric acute lymphoblastic leukemia susceptibility. Nature 2014;75(6):767–73. doi:10.1038/pr.201443.

[19] Liu B, Wang T, Jiang J, Li M, Ma W, Wu H, et al. Association of BET1L and TNRC6B with uterine leiomyoma risk and its relevant clinical features in Han Chinese population. Sci Rep 2018;8(1):7401. doi:10.1038/s41598-018-25792-z.